

The glycerol stabilized calcium phosphate cluster for rapid remineralization of tooth enamel by a water-triggered transformation

Nan Luo^{1,2#}, Bing-Qiang Lu^{3##}, Yu-Wei Deng^{2,4}, Hua Zeng³, Yu Zhang^{1,2}, Jing-Yu Zhan^{1,2}, Xiao-Chen Xu^{1,2}, Gui-Zhi Cao², Jin Wen^{2,4}, Zhiyuan Zhang^{2,5}, Xi-Ping Feng^{1,2}, Xinquan Jiang^{2,4}, Feng Chen^{3*}, Xi Chen^{1,2*}

Affiliations

¹: Department of Preventive Dentistry, Shanghai Ninth People's Hospital, Shanghai Jiao Tong University School of Medicine, Shanghai, 200011, P. R. China

²: College of Stomatology, Shanghai Jiao Tong University; National Center for Stomatology; National Clinical Research Center for Oral Diseases; Shanghai Key Laboratory of Stomatology, Shanghai Research Institute of Stomatology, Shanghai, 200011, P. R. China

³: Center for Orthopaedic Science and Translational Medicine, Department of Orthopedic, Spinal Pain Research Institute, Shanghai Tenth People's Hospital, School of Medicine, Tongji University, Shanghai, 200072, P. R. China

⁴: Department of Prosthodontics, Shanghai Ninth People's Hospital, Shanghai Jiao Tong University School of Medicine; Shanghai Engineering Research Center of Advanced Dental Technology and Materials, Shanghai, 200011, P. R. China

⁵: Department of Oral and Maxillofacial-Head Neck Oncology, Shanghai Ninth People's Hospital, Shanghai Jiao Tong University School of Medicine, Shanghai, 200011, P. R. China

#: These authors contributed equally.

Corresponding Authors

*E-mail: bqlu@tongji.edu.cn

*E-mail: fchen@tongji.edu.cn

*E-mail: chenx1853@sh9hospital.org.cn

Abstract

Using remineralization materials to grow hydroxyapatite (HAP) crystals on the surfaces is a common strategy for the repair of early demineralized tooth enamels. As the efficacy is often impaired by harsh dynamic oral environments, e.g., continuous flow of saliva and friction of moving maxillofacial muscles, a rapid remineralization is expected to avoid or diminish these influences. But there has been a great dilemma to address this expectation, as the stabilizers used for preparation and storage of these materials, in turn, could resist their transformation during remineralization. Here, by dissolving the ions of calcium and phosphate in mixed solvents of glycerol and water, we found a stable species with ultrasmall size (1-2 nm), termed glycerol stabilized calcium phosphate cluster (GCPC), which can perform a fast enamel repair via the water-triggered transformation in both static or dynamic environments. The high permeability and water-responsive character allow GCPC to easily enter the nano-/micro-sized enamel defect sites and transform into HAP nanorods immediately, going through a special intermediate—amorphous calcium phosphate nanowire, whose subsequent crystallization product (the nanorods) stands vertically to them and enamel surface. Both in vitro and in vivo studies display that, GCPC forms a compact HAP repair layer within a short time (30 min), which is much faster than the conventional materials (hours or days), and recovers mechanical properties to the values close to those of sound enamel. Moreover, a double-blind, randomized, crossover clinical trial based on in situ model further demonstrates an excellent remineralization efficiency of GCPC in the real human oral environment. Given its rapid repair capacity, simple preparation process, low cost and remarkable biocompatibility, GCPC is promising for large-scale preparation and clinical applications in dental remineralization.

Main

Loss of tooth tissues by demineralization or trauma is one of the most negative effectors on life quality, causing health problems and economic burdens throughout the world¹. As an outstanding biomineralization work in nature, human tooth enamel forms via a programmed series of cellular and biochemical regulations². Due to the irreproducible enamel development microenvironment after tooth eruption, enamel is scarcely self-repaired if damaged^{3,4}. For example, the cavity caused by dental caries normally progresses continuously without reverse, and ultimately impairs underlying dentin, even the pulp. Until now, a variety of materials such as fluoride⁵, casein phosphopeptide (CPP)⁶, amelogenin mimics⁷ and calcium phosphates^{8,9} have been explored to remineralize enamels by promoting the growth of fluor-/hydroxyapatite (HAP). Generally, a complex procedure of pre-treatment and a mild static environment during treatment are required to achieve an ideal outcome. Despite this, the repair efficacy of these materials is still weakened by low rate. For example, the tooth interface should be dried first, then coated with the materials followed by dried again, and finally incubated in static artificial saliva for a long time to induce transformations of the applied materials or the precipitation of apatite crystals^{7,8,10}. The real oral environments, in contrast, are much harsher since the sustained flow of liquid in the mouth and friction on the tooth surface may lead to the detachment of materials detached from enamels before finishing the repairs. Therefore, a rapid repair rate in harsh dynamic environments is desired to avoid or diminish these influences for more effective enamel remineralization.

The human tooth enamel is highly patterned and consists of tightly packed arrays of HAP nanorods that organize into an intricate interwoven structure³. While originating from calcium and phosphate ions, the HAP formation in solutions involves various intermediate species ranging from pre-nucleation ones (e.g., prenucleation cluster¹¹⁻¹³, liquid precursor^{14,15}, ion dense liquid¹⁶) to post-nucleation ones (e.g., amorphous nanocluster^{17,18}, amorphous nanoparticle¹⁹, nanocrystal^{20,21}). Theoretically, each one can be potentially used to build the targeted complex structures. In fact, it is believed that their formation, growth, assembly and phase transformation are tuned by cells and secreted substances in animals to form the hard tissues with delicate structures and strong mechanical properties^{3,22}. This has inspired researchers to repair the enamel defects based on specific intermediate species^{8,23-25}, but the resultant structures are often distinct from native enamels, or the repairs take long time due to low transformation rates. For a rapid remineralization, the used materials should quickly adhere to the enamel surface, then permeate into the nano-/micro-sized interstices, and transform into HAP nanorods in saliva within a short time. However, a dilemma arises: stabilizers are required to capture the intermediate state during synthesis and storage of these materials, but their transformations are unexpectedly inhibited by stabilizers when treating enamel defects.

In this study, we have developed an intermediate species in mixed solvents of glycerol and water, denoted as glycerol stabilized calcium phosphate cluster (GCPC), to address this challenge. Glycerol is widely used in biomedicine, food industry, cosmetics and oral products owing to remarkable biocompatibility^{26,27}. With high molecular polarity, glycerol is able to solubilize a variety of polar molecules and inorganic salts. Besides, given its big size and high affinity to various cations (e.g., Ca^{2+}) via the ternary-hydroxy groups, glycerol can effectively retard the transformation and aggregation of the substances formed in it, which is beneficial for obtaining the early state species during their evolution. When contacting aqueous solution (e.g.,

saliva), water molecules rapidly exchange with glycerol, disturbing the stability of the GCPC and inducing assembly and transformation. Indeed, our studies find that, GCPC, with a very small size (1-2 nm) and high stability in mixed solvents of glycerol and water, is able to remineralize the acid etched enamels rapidly in a water-triggered way: on enamel, it can easily enter the nano-/micro-sized defect sites and transforms into HAP nanorods immediately going through a special intermediate—amorphous calcium phosphate nanowire. Both in vivo and in vitro, GCPC restores enamel mechanical properties by forming a dense mineral repair layer in static or dynamic saliva. This character effectively avoids the impact of the dynamic environments in oral, which provides an enlightening foundation for the efficient repair of damaged enamels.

Results and discussions

The preparation and characterization of GCPC

GCPC was obtained in a solution of Ca^{2+} and PO_4^{3-} ions dissolved in the mixed solvents of glycerol and water. As a polar solvent, glycerol is able to dissolve Ca^{2+} and PO_4^{3-} salts, but inhibits their reaction into calcium phosphate precipitations, which differs from water solvent. Indeed, as shown in **Fig. 1A**, the glycerol solution containing 0.050 mol/L Ca^{2+} and 0.033 mol/L PO_4^{3-} ions displays very weak turbidity and its OD value has no significant difference from that of pure glycerol (**Fig. S1**), indicating that rare mineral species are yielded, which is varied from the manifest white precipitation formed in the aqueous solution. When water is introduced into the glycerol solutions while maintaining the ion concentrations, it distinctly turns into turbid (**Fig. S1A-C**) and the turbidity is improved with the increase of water content (volume content of water in solvents is from 1.67 to 16.7 v/v%), consistent with the rise of the OD values (from 0.053 to 0.13) in **Fig. S1F**. On liquid nuclear magnetic resonance (NMR) spectra (**Fig. 1B**), the solution of free PO_4^{3-} ions (from Na_3PO_4) in mixed solvents (water content 16.7 v/v%) corresponds to a sharp resonance at 3.2 ppm, but a broader one in the range of -15~15 ppm arises along with the sharp one significantly weakened and shifted (to 2.8 ppm) when Ca^{2+} ions (from CaCl_2) are added. These all indicate that the solutions of Ca^{2+} and PO_4^{3-} ions form new species in the mixed solvents of glycerol and water. Besides, when tripling the concentration of Ca^{2+} and PO_4^{3-} ions (to 0.15 and 0.10 mol/L, respectively, termed 3X-GCPC), a more turbid (also higher OD value) but still stable solution is obtained (**Fig. S1D**), where no significant phase separation is observed even under centrifuge of 10000 rpm for 1 min, suggesting a high solubility of the formed species that correspond to the turbidity.

Liquid cell TEM is capable of in situ monitoring species in the solutions, which avoids the negative effects by the drying operation required for the conventional TEM observation²⁸. This technology was applied to elucidate the morphology of the formed species in mixed solvents. Here, the solution Ca^{2+} and PO_4^{3-} ions with volume content of water in solvents 16.7 v/v% was characterized using a spherical aberration corrected transmission electron microscope (ACTEM) equipped with a liquid cell holder. As shown in **Fig. 1C**, clusters with dark contrast in the size of 1-2 nm are observed (labeled with squares) in the solution, which are denoted as glycerol stabilized calcium phosphate clusters (GCPCs) due to the essential stabilizing effect by glycerol as discussed in the following. Previously, calcium phosphate clusters have been reported in aqueous¹³ or organic solutions²⁹. In general, bare clusters are extremely unstable and tend to aggregate into bigger particles or even chemically transform immediately after formation.

Establishing stabilizers on their surfaces is required to avoid this, however, they may in turn impair the intended assembly and transformation of the clusters when building the target structures.

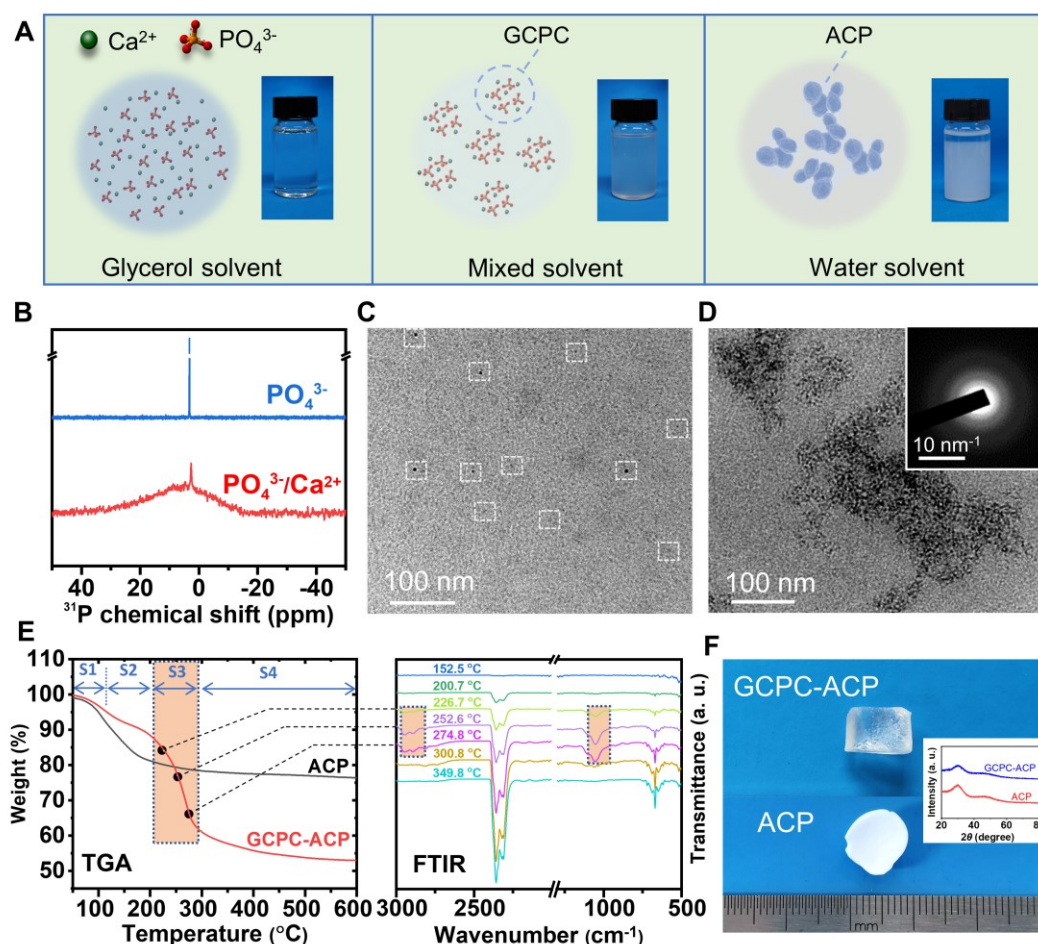


Fig. 1. Synthesis and characterization of GCPC. (A) Schematic and digital images of the prepared solutions by adding the same concentration of $\text{PO}_4^{3-}/\text{Ca}^{2+}$ ions in different solvents (glycerol, mixed (glycerol + water, water content 16.7 v/v%) and water solvents). (B) ^{31}P NMR spectra of the solutions containing PO_4^{3-} ions or $\text{PO}_4^{3-}/\text{Ca}^{2+}$ ions in mixed solvents (water content 16.7 v/v%). (C) Liquid cell TEM image of GCPC in the solution of mixed solvents (water content 16.7 v/v%). White dashed squares highlight the GCPCs on the image. (D) TEM image of GCPC-ACP formed by adding GCPC into a large amount of ethanol. Inset: SAED pattern. (E) TGA-FTIR analysis of ACP and GCPC-ACP by which FTIR spectra (right) of the gas released during heating the sample for TGA (left) is collected simultaneously. The TGA curve of GCPC-ACP displays four stages (labeled as S1-S4). The selected FTIR spectra (recorded at 226.7-274.8 °C) of S3 show characteristic bands at 2948, 2894 and 1054 cm^{-1} marked with rectangles, indicating that this stage corresponds to the loss of glycerol. Therefore, the contents of water and glycerol are calculated to be 8.37 wt% and 23.3 wt%, respectively. (F) Digital images of dried GCPC-ACP (top) and normal ACP (bottom) prepared in water displaying a high transparency and an opaque white, respectively. Inset: XRD spectra revealing the amorphous phases of GCPC-ACP and ACP.

In our strategy, the aggregation and transformation of GCPC are effectively inhibited by glycerol through its large size and high affinity of the ternary hydroxyl group to Ca^{2+} ions, but can be induced by replacing glycerol with a certain substance, e.g., water. Indeed, we find that the prepared GCPC shows very high stability. During observing GCPC with ACTEM in liquid cell, no morphological changes were found, which also corroborates that this species is not a byproduct of electronic beam irradiation. Besides, the GCPC solution (water content 16.7 v/v%) can keep a homogeneous state without visible phase separation for at least 2 weeks (**Fig. S1E**). However, when being dispersed in a large amount of water (1 mL GCPC in 10 mL water), where the glycerol exchanges with water molecules driven by the high mutual solubility of glycerol and water, precipitation is immediately formed, which turns out to be ACP nanoparticles according to TEM, selected area electronic diffraction (SEAD) characterizations (**Fig. S2**). This ACP will further crystallize in aqueous solutions as discussed below. The results suggest that, although possessing high stability, GCPC can undergo a rapid conversion by the induction of water, which is termed the water-triggered transformation in this paper.

When mixing GCPC with methanol, ethanol or ethylene glycol at a volume ratio of 1:10 to exchange glycerol with each of them, solid precipitation occurs immediately (**Fig. S3**). This suggests that these organic alcohols cannot stabilize GCPC, and glycerol is specifically required for it. The precipitation yielded by mixing GCPC with ethanol (denoted as GCPC-ACP) was characterized. As shown in **Fig. 1D**, it displays a morphology of aggregated clusters with amorphous phase (according to SAED pattern in **Fig. 1D inset**), which also corroborates the cluster morphology of GCPC. Thermogravimetric-Fourier transform infrared spectrum (TGA-FTIR) analysis (**Fig. 1E**) was used to further characterize GCPC-ACP, by which FTIR spectra of the gas released during heating the sample for TGA is collected simultaneously. In addition to water (8.37 wt%), a high content of glycerol (23.3 wt%) is determined in GCPC-ACP as well. As this sample was washed with ethanol for 6 times, and thoroughly dried in vacuum, it is reasonable to speculate that, like water, glycerol molecules are incorporated in GCPC-ACP rather than weakly adsorbed on its surface. This also indicates that, glycerol has a strong interaction with GCPC in the mixed solvents, which thus contributes to their high stability as discussed above. Interestingly, the dried GCPC-ACP displays a monolith with a high transparency (**Fig. 1F**), which is different from the white color of normal ACP prepared in water and previously reported ACP powders³⁰, indicating a high structural continuity with the constituent particles highly compacted or fused³¹.

Repair of demineralized enamel in vitro

GCPC was further applied in enamel remineralization to explore its application in dentistry. Here, GCPC in the mixed solvents (termed GCPC solution or 3X-GCPC solution as described in experimental section), where it forms, is directly used for the following studies. In our study, GCPC is advantageous in 3 aspects: (1) highly concentrated constituent ions of calcium phosphate in the solution (e.g., up to Ca^{2+} 0.15 mol/L, PO_4^{3-} 0.10 mol/L for the 3X-GCPC solution, comparing to 0.01-0.02 mol/L of them in (simulated) body fluids) without forming precipitation or big solid particles; (2) high fluidity and permeability endowed by its small size; (3) high stability and water-triggered transformation favoring both long-term storage and rapid repair.

Cytotoxicity of GCPC was first tested upon human oral keratinocytes (HOKs) and human

dental pulp stem cells (DPSCs) with CCK-8 assay and Live/dead staining. For each kind of cell (HOKs or DPSCs), the CCK-8 assay shows very little difference of the cell proliferations between the GCPC group (incubation of cells with GCPC) and control (incubation of cells without GCPC or other materials) after 1 d and 2 d (**Fig. S4A and B**). The GCPC exhibits excellent biocompatibility even at a high concentration (50 mg/mL). The live/dead staining experiment further confirms the results, showing that both HOKs and DPSCs have high viability at 2 d in different concentrations of the GCPC (**Fig. S4C**). As glycerol, Ca^{2+} and PO_4^{3-} ions are rich in the human bodies, it is reasonable to understand the excellent biocompatibility of GCPC, which is also essential for its applications in biomedicine.

For an in vitro study, a caries model was made by etching the sound enamel with 37wt% phosphoric acid for 60 s. SEM micrographs show that the smooth surface of sound enamel (**Fig. S5**) changes into rough and porous with HAP nanorod crystals loosely arranged on it as a result of HAP dissolution in acid environment (**Fig. 2A-A2**). The remineralization of enamel was subsequently demonstrated on this model caries. After being totally wetted by artificial saliva, a drop of GCPC solution was added onto it using a micro brush (brushing for 5 s) (schematic in **Fig. 2A3**), then immediately immersed in artificial saliva and incubated for a certain duration. Owing to the small size, GCPC can easily enter the nano-/micro-sized interstices of the defects. Afterwards, they rapidly assemble and transform so as to remineralize the defects during the dissolving of glycerol in artificial saliva. As expected, SEM micrographs show that the newly formed materials, which should be originated from GCPC in artificial saliva, densely fill in the defect sites at a very early stage (5 min) (**Fig. 2B-B3**). Magnified micrographs reveal that the materials are composed of highly packed and well-defined nanowires with a diameter of 5-10 nm and length of up to hundreds of nanometers. TEM micrograph confirms the morphology of nanowires (**Fig. S6**), and further suggests an amorphous phase by the SAED pattern (inset of **Fig. S6**).

Over incubation time, the network of nanowires remains on the enamel surface at 10 min, but becomes more compact as more nanowires are generated (**Fig. 2C**). Moreover, the knots formed by fusion of the nanowires are observed (marked by dashed circles in the inset of **Fig. 2C1 and C2**), which should be the beginning of a further transformation (schematic in **Fig. 2C3**). Notably, the knot with elongated shape is vertical to the enamel surface (also the ACP nanowires). By 30 minutes, the nanowires have completely converted into hydroxyapatite nanorods with a diameter of 20-50 nm and length of 100-300 nm (**Fig. 2D-D3**), resembling those of native enamels³. The significant repair effect is also evidenced by a distinct contrast difference between GCPC treatment area and GCPC non-treatment area (schematic is shown in **Fig. S7A**) on each etched enamel, where the boundary is marked with an arrow in inset of **Fig. 2D**. As a comparison, the remineralization capacity of CPP-ACP paste, a normal commercial enamel remineralization product in clinic, is also tested on the caries model for the same time (30 min). Unlike GCPC, the morphology of CPP-ACP treatment area shows little difference from that of CPP-ACP free one (**Fig. S7B**, the boundary is marked with an arrow in inset). Attributed to the weak repair effect in such short time, only sparse minerals adhere to the enamel (**Fig. S7C**). In addition, applying the 3X-GCPC leads to a very flat, well-organized and more compact repair layer at 30 min (**Fig. S8**), indicating that a higher concentration of the GCPC can improve the repair effect in vitro. We note that, the surfaces of all GCPC treated enamels are flushed by ethanol before SEM characterizations, indicating that the species

formed by GCPC conversion strongly adhere onto the enamels even at very early stage.

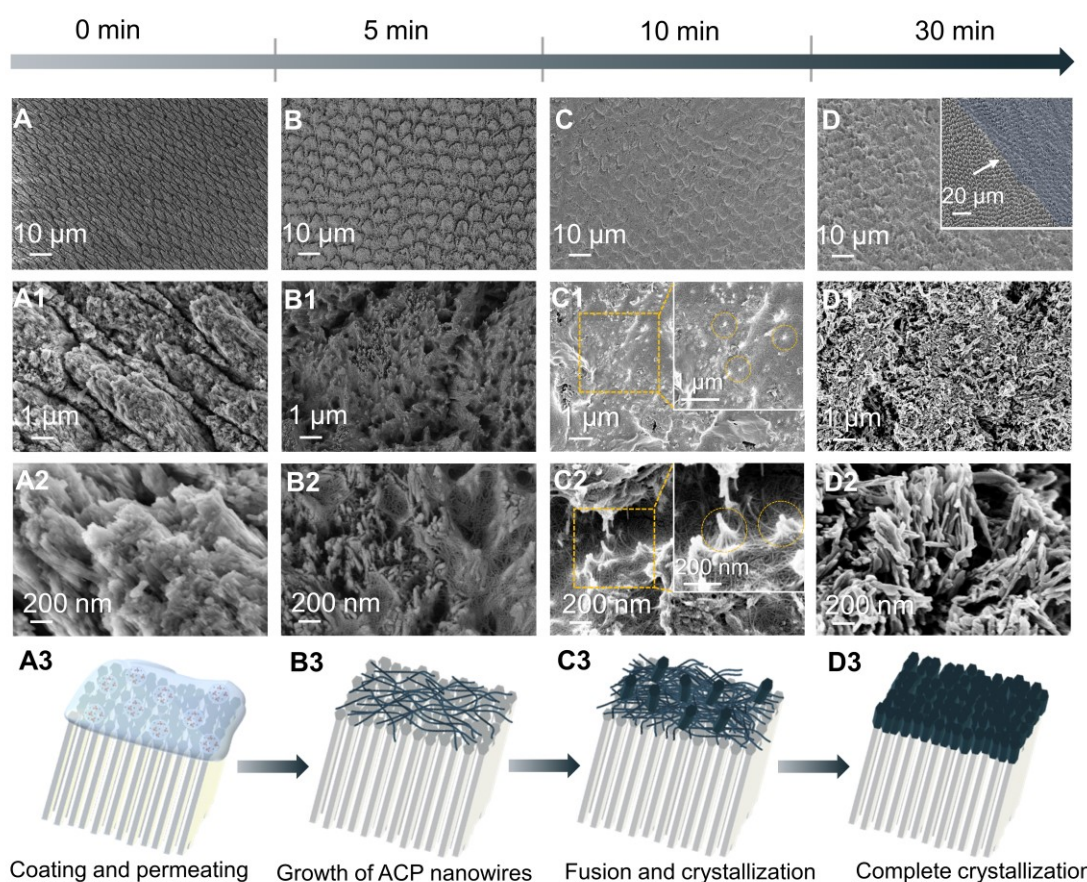


Fig. 2. Rapid repair of demineralized enamel using GCPC. (A-A2, B-B2, C-C2, D-D2) SEM images of the top surface of etched enamel before (A-A2) and after treatment for 5 min (B-B2), 10 min (C-C2) and 30 min (D-D2). Insets of (C) show high-magnification images of the square selected areas. The knots marked by yellow dashed circles reveal that HAP nanorods are formed by fusion of the nanowires. The obvious boundary between GCPC treatment area (blue region) and GCPC non-treatment area on enamel is marked by an arrow in inset of (D). (A3, B3, C3, D3) schematics illustrating the repair performances of GCPC on etched enamels over time, which goes through the coating and permeating in 0 min (A3), growth of nanowires in 5 min (B3), fusion and crystallization in 10 min (C3) and complete crystallization in 30 min (D3).

Based on the characterizations above, we propose a pathway of enamel repair by GCPC (**Fig. 3**). When coating GCPC on the acid etched enamel, they quickly permeate into the nano-/micro-sized defects. Meanwhile, in the artificial saliva environment, glycerol, which acts as a stabilizer in GCPC, is dissolved instantly, resulting in the formation of ACP. As a result of the interaction between GCPC and enamel substrate, the growth of ACP is highly oriented, leading to the morphology of nanowires (diameter 5-10 nm). Subsequently, the ACP nanowires fuse and crystallize into HAP nanorods (diameter 20-50 nm). These rod nanocrystals, as the constituent units of the repair layer, grow closely on the enamel surface. The mineral formation indicates a nonclassical crystallization behavior, i.e., the crystals grow by aggregation of particles rather than ion-by-ion attachment (classical crystallization), which has been widely accepted for the growth of biominerals³²⁻³⁴. Interestingly, in this study, the GCPCs do not

aggregate and crystallize into HAP nanorods directly, but go through an intermediate form—ACP nanowire. It is conventionally believed that amorphous solids can hardly grow into highly elongated morphologies without external regulations (e.g., templates) due to the isotropic microstructure^{35,36}. Since we did not find such morphologies by directly mixing GCPC with artificial saliva or pure water, whereby the possible effect of glycerol as an amphiphile surfactant is excluded, it is reasonable to hypothesize that the amorphous nanowire formation occurs via the interaction between GCPC and the specific substrate (i.e., HAP nanocrystals of enamel) in artificial saliva. This is consistent with a finding that, on a disk surface of HAP nanorods (see preparation details in experimental section), similar nanowires are formed as well (**Fig. S9A and B**); but on glass, only nanoparticles are observed (**Fig. S9C and D**).

We note this remineralization behavior could expand the theory of nonclassical crystallization, for the following reasons. First, while it has been established that crystalline substrates can induce oriented growth of biomineral crystals by attaching amorphous nanoparticles^{8,37,38}, but the formation of ACP nanowires (especially with such high aspect ratio) on it is unprecedented, as the isotropic microstructure of ACP does not encourage the oriented growth. Second, during the growth of HAP crystals from ions or clusters in the absence of surfactants, ACP nanowire has never been found as an intermediate before. Third, the subsequent crystallization of ACP nanowires grows the nanorods vertical to them (not parallel), indicating that ACP nanowires do not act as the templates for crystals to grow following their shapes.

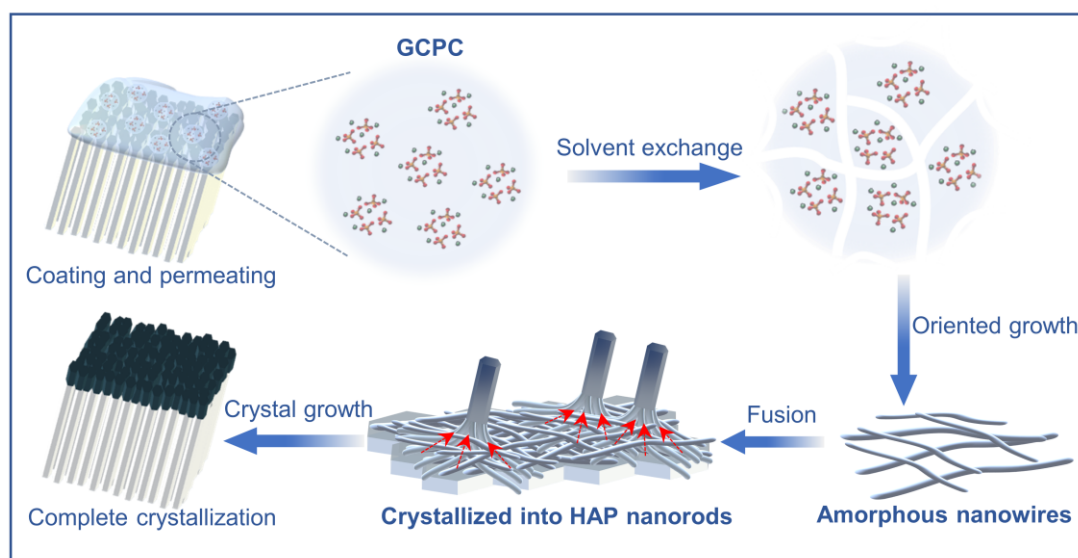


Fig. 3. Schematic of the rapid repair process of demineralized enamel by GCPC via a water-triggered transformation.

With the incubation time prolonged to 24 h, the repaired layer has no significant changes from that of 30 min, indicating that such short time (30 min) is sufficient for GCPC to complete its repair process (**Fig. 4A-C**). Side view of the treated enamel shows that the thickness of the remineralization layer is $\sim 1 \mu\text{m}$ (**Fig. 4C**), and validates the continuity and structural integration on the boundary between enamel and the repaired layer (**Fig. 4B**). Notably, when the etched enamel without coating GCPC is directly immersed in artificial saliva, no visible HAP crystal

growth is found, indicating that artificial saliva has very weak capacity of enamel remineralization, and excluding the possibility of the enamel remineralization by artificial saliva independently during GCPC treatment (**Fig. S10A and B**). Further treating the enamel with GCPC again and culturing in artificial saliva one more day through the same procedure (i.e., treatment with GCPC for 2 times, and incubation in artificial saliva for 48 h totally) (**Fig. 4D-F**), a thicker remineralization layer (3~4 μm) composed of HAP nanorods are formed (**Fig. 4F**). This indicates that repeating the treatment with GCPC can also improve the remineralization effect.

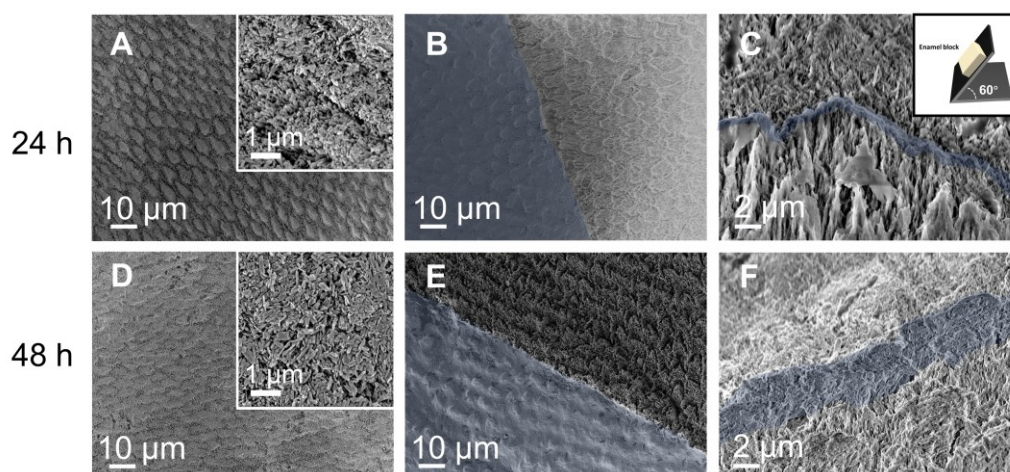


Fig. 4. Repair of demineralized enamel using GCPC for 24 h and 48 h. (A-C) SEM images of GCPC treatment areas (A), boundary between GCPC treatment (blue) and non-treatment areas (B), and the cross section (C, blue region: section of the repair layer) on etched enamel after repair for 24 h. Inset in (C) shows that the enamel sample is tilted to a degree of 60° for side observation. (D-F) SEM images of the GCPC treatment areas (D), boundary between GCPC treatment (blue) and non-treatment areas (E), and the cross section (F, blue region: section of the repair layer) on etched enamel after repair for 48 h.

Since the teeth in mouth are surrounded by fluid saliva, and frequently rubbed by moving cheek and tongue, we simulated the dynamic environment in mouth to further evaluate the repair capacity of GCPC. Here, based on treatment process as above, GCPC coated samples are placed under oscillation condition (80 rpm/min) during incubating in artificial saliva. SEM images show that a dense repair layer composed of short HAP rods still forms on enamel surface in such a harsh environment within either a short (30 min) or long (24 h and 48 h) mineralization time (**Fig. 5A-F**). These results suggest that GCPC has a high repair efficiency in both static and dynamic environments.

As mechanical properties, especially hardness, are major contributors to normal functions of teeth, thus it is essential to evaluate it on the repaired enamels. **Fig. 5G and H** illustrate the microhardness of the sound, acid etched (caries model) and GCPC repaired enamels characterized by a Knoop microhardness tester. The sound enamel has a hardness of 363.83 ± 5.66 HV (mean \pm SD), but it is significantly weakened after acid etching with the value reduced to 197.33 ± 20.44 HV. Whereas, after a fast repair (30 min), the treatments by GCPC and 3X-

GCPC greatly recover the hardness to 298.73 ± 20.34 HV and 305.67 ± 21.31 HV, which are 82.1% and 84.0% of sound enamel, respectively. These mechanical property recoveries should be attributed to the growth of compact HAP nanorods on etched enamel by remineralization. In contrast, by using conventional remineralization agents, e.g., 2wt% NaF and CPP-ACP paste, for the same duration (30 min), the enamel hardness stays at relatively low values of 253.07 ± 13.94 HV and 253.87 ± 14.88 HV because of their poor remineralization rates. The hardness of the enamel is further improved after incubation for 24 h. Compared to 2wt% NaF (266.07 ± 5.60 HV) and CPP-ACP paste (291.43 ± 7.11 HV), the hardness of the repaired enamel by GCPC and 3X-GCPC increases to 322.73 ± 4.99 HV (88.70% of sound enamel) and 328.30 ± 6.97 HV (90.23% of sound enamel), respectively. In addition, GCPC treated enamel also shows prominent hardness recovery under oscillation conditions that mimics the hash dynamic oral environment. At 30 min, the hardness of enamel (Harsh GCPC in **Fig. 5G**) repaired in oscillator reaches to 287.90 ± 12.19 HV (79.13% of sound enamel); after 24 h, the value reaches to 331.90 ± 14.41 HV (91.22% of sound enamel), the highest of among all samples.

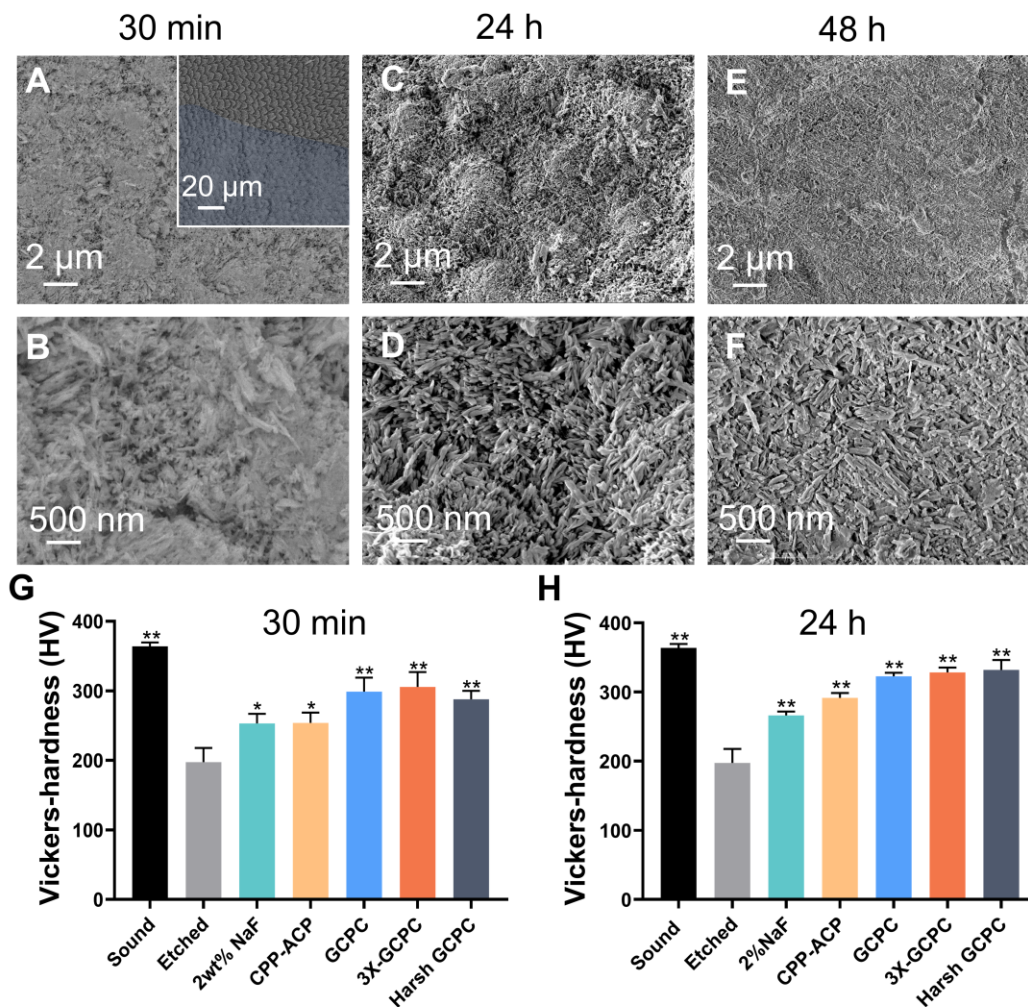


Fig. 5. Repair of demineralized enamel using GCPC in harsh environment. (A-F) SEM images of the enamel repaired by GCPC under oscillation condition (80 rpm/min) for 30 min (A, B), 24 h (C, D) and 48 h (E, F). Inset: the boundary between GCPC treatment (blue) and non-

treatment areas. (G, H) Microhardness of different enamel samples after repair for 30 min (G) and 24 h (H). Sound, etched, 2wt% NaF, CPP-ACP, GCPC, and 3X-GCPC correspond to the samples of sound enamel, etched enamel (blank group), enamels repaired by 2wt% NaF, CPP-ACP paste, GCPC and 3X-GCPC in static artificial saliva respectively; Harsh GCPC represents the enamel repaired by GCPC under oscillation condition. The error bars represent the mean \pm SD for n = 3, *p < 0.05, **p < 0.01.

Table 1. Comparison of GCPC with the representative materials explored for enamel remineralization in the past 10 years. AS: artificial saliva, SBF: simulated body fluid, Glu: glutamic acid, MMP-20: matrix metalloproteinase-20, CS-AMEL: hydrogel system composed of chitosan-amelogenin, PCBAA: zwitterionic poly-(carboxybetaine acrylamide).

Year	Repair materials	Pre-treatment (before immersed in AS /SBF)	Time for significant remineralization*	Thickness of the repaired layers
2011 ⁹	Glu-Directed assembly of apatite nanoparticles	Coat the material on enamel, then wash with ethanol and dry in air at 25 °C	72 h, the particles turned into rod-like apatite crystals	0.6~1 μ m in 3d
2017 ²³	Chimaeric-peptide-guided ACP nanoparticles	Coat the material on enamel, then brush for 10 min	7 d, a layer of ordered enamel-like crystals was formed	No data
2018 ³⁹	MMP-20/CS-AMEL hydrogel	Coat the material on enamel, then keep in a desiccator for 15 min	5 d, needle-like HAP crystals were formed	No data
2019 ⁸	Calcium phosphate ion clusters	Coat the material on enamel, then dry in air for 15 min	48 h, the coated material formed a well-crystallized HAP layer	2.0~2.8 μ m
2020 ⁷	Amyloid-like amelogenin mimics	Immerse the enamel in the solution containing the material for 10 min	7 d, a layer of the rod-like HAP crystals was formed	2.0~2.8 μ m
2021 ⁴⁰	Biomimetic enamel matrix proteins	Coat the material on enamel, crosslink it, then dry in air	24 h, the prismatic and interprismatic structures were restored with newly formed HAP crystals	2 μ m
2022 ¹⁰	Low-complexity protein segments	Immerse the enamel in a solution containing the material for 12 h, then wash with water and dry in air	3 d, initial formation of a new HAP layer	4.6 and 5.1 μ m in 6 d

2022 ²⁴	PCBAA/ACP nanocomposite	Coat the enamel with fresh material	1 d, interprismatic zones were almost filled with the newly formed HAP crystals	10.5 μm in 7 d
This work	GCPC	Brush the enamel for 5 s during material coating	30 min, the coated material completely transformed into compact HAP nanorods	3~4 μm in 2 d

*: Here we present the earliest time points when the adsorbed materials on the enamels completely transformed into apatite crystals, or induced the formation of apatite crystals.

Table 1 summarizes the representative advances on enamel remineralization materials in the past 10 years, where the details of their repair performance are compared with GCPC. Among these materials, application of GCPC shows apparent advantages of rapid rate (within 30 min), effectiveness in harsh environment and easy conduct (no need for special pretreatment of enamels). Considering in the clinic practice of enamel repair, there's no need for patients to dry the tooth surface, spent additional time for material adhering, or limit too much mouth motion, these merits are beneficial for positive patient compliance and clinical promotion.

Animal study of enamel repair

Encouraged by the above results, we further applied an *in vivo* animal model (**Fig. 6A**) to ascertain the performance of the GCPC on remineralization of etched enamel by a rapidly water-triggered transformation. In our animal model, acid etched enamel blocks with half surface coated with nail varnish were fixed in the maxilla of rats where they were under the frictions from buccal and lingual muscles. Moreover, the mouths of rats provided a dynamic liquid environment containing both inorganic ions and organic molecules (**Fig. 6B**). Without any additional pretreatments of enamels, we used micro brushes to apply GCPC, CPP-ACP paste or deionized water (blank) on enamel blocks to mimic daily oral care, then evaluate the repair effects after a certain time.

After 30 min of oral incubation, hardly any new crystals grow on the demineralized enamels treated with deionized water (**Fig. 6D, Fig. S11A and B**), leading to little differences between the treated and un-treated areas. This indicates that the enamel defects could not be repaired by saliva alone in such a short time. Instead, GCPC and CPP-ACP paste treatments result in remineralization effects on the surfaces, and that of GCPC forms much more compact crystals than CPP-ACP paste (**Fig. 6E and F, Fig. S11E, F, I and J**). These crystals have the morphologies of nanorods with a diameter of 50-70 nm and length of 100-300 nm. This proves that, like *in vitro* performance, GCPC also has a rapid repair ability *in vivo* via the water-triggered transformation. In contrast, CPP-ACP paste should be relatively more vulnerable than GCPC to dynamic environment of the actual mouth due to the slow repair rate. After 24 h, similar to the early stage, we can observe the densest repair layer composed of HAP nanorods on the GCPC group than the others (**Fig. 6I, Fig. S11K and L**). Meanwhile, deionized water (**Fig. 6G, Fig. S11C and D**) and CPP-ACP paste (**Fig. 6H, Fig. S11G and H**) groups still

present little difference of the morphology from the etched enamel.

Contributed by the high performance of remineralization, GCPC group shows a great enamel hardness recovery in 30 min, reaching the value to 280.57 ± 6.70 HV, compared with deionized water (207.53 ± 14.07 HV) and CPP-ACP paste (253.50 ± 4.73 HV) groups. Further mechanical measurements at 24 h also show that the hardness of GCPC group (340.13 ± 17.10 HV) is the highest among the characterized groups (CPP-ACP paste group: 293.47 ± 11.35 HV; deionized group: 222.73 ± 25.24 HV. **Fig. 6C**). These results confirm that the remineralization by GCPC does not only recover the structure of enamels, but also its mechanical properties within very short time.

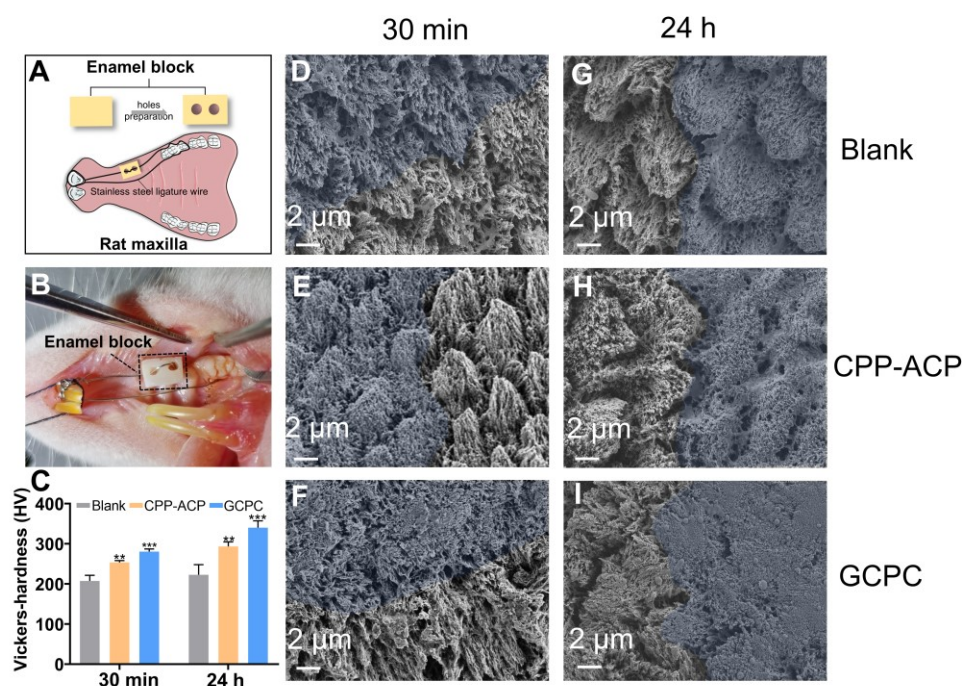


Fig. 6. The repair of demineralized enamel in vivo. (A, B) Schematic (A) and photograph (B) of vivo animal model showing the etched enamel fixed in the oral cavity of rats. (C) Microhardness of the enamels repaired by different materials in vivo for 30 min and 24 h. The error bars represent the mean \pm SD for $n = 3$, ** $p < 0.01$, *** $p < 0.001$. (D-F) SEM images of the enamels repaired by deionized water (D), CPP-ACP paste (E) and GCPC (F) for 30 min in vivo. (G-I) SEM images of the enamels repaired by deionized water (G), CPP-ACP paste (H) and GCPC (I) for 24 h in vivo. The blue regions represent the treatment areas.

Clinical trials of enamel repair

A double-blind, randomized and crossover in situ clinical trial was conducted to investigate the performance of GCPC on enamel remineralization in human mouths. In this study, demineralized enamel blocks were attached to removable occlusal splints as an in situ model (the schematic is shown in **Fig. 7A**), which have the following advantages: protection of participants' natural teeth; consistency of treatment conditions among enamel specimens; favoring the in vitro measurements due to the removability of enamel specimens from occlusal splints⁴¹. The GCPC used for clinical trials was prepared as above with a slight modification to lower the pH of GCPC in water from 9.1 to 7.5 (see experimental section) although the previous

one did not show any negative effects during cell and animal tests. Prior to clinical trials, necessary toxicity tests including cytotoxicity (**Fig. S12**) and histopathological test (**Fig. S13**) were performed to further confirm the safety of the used GCPC. Six participants (one male and five females, age 23–26 years) were recruited for clinical trials and all completed the treatments with three agents for each one: GCPC, CPP-ACP paste and control in different sequences (see Experimental section). There were no significant adverse events reported during the study.

In the return visit, all participants indicated that they had no discomfort with any test solutions and that their taste and texture were acceptable. Furthermore, organoleptic test of all agents was assessed by participants before unblinding, and that of GCPC is present in **Fig. 7B**. From the overall result, participants are very satisfied (score = 5.00) with mucosal comfort level of GCPC and satisfied with their performance in transient taste alteration (score = 4.67) and oral humidity (score = 4.50). Although no additional flavor substances are added in GCPC, the taste (score = 3.67) and texture (score = 4.67) of GCPC still obtain high satisfaction.

The microhardness result of all participants is shown in **Fig. 7C**, where the value of each treatment is calculated by averaging those of all participants. The enamel specimens of GCPC group at 30 min have the highest hardness, reaching to 254.38 ± 25.05 HV, which is significantly superior to CPP-ACP group (217.03 ± 20.91 HV) and control group (209.71 ± 20.16 HV). In comparison, there is no significant difference between CPP-ACP group and control group ($p=1.00$), which varies from the results of in vitro and animal experiments. At 24 h, the hardness of CPP-ACP group and control group are 238.60 ± 26.95 HV and 219.28 ± 29.65 HV, respectively, again displaying no significant difference. However, as expected, GCPC group still has the significantly highest hardness in these three, reaching to 267.93 ± 27.76 HV. In order to learn more details of the repair performances, microhardness result of individual participant is further analyzed one by one (**Fig. 7D**). At either 30 min or 24 h, hardness value of the GCPC group of 4 participants (among 6) are higher than that of the control group. These results confirm the remineralization effectiveness of GCPC in most of the participants.

SEM results show that, at either 30 min or 24 h, repaired enamel surface of GCPC group form more dense minerals, and displays smoother than the other groups (**Fig. 7E-J**). This is consistent with the microhardness result, as the formation of more minerals on the enamel can lead to better recovery of the enamel hardness. Altogether, the clinical trial proves a rapid restorative effect by GCPC in real human oral environment within short time (30 min or 24 h).

In the clinical practice, remineralization agents are expected to function within the shortest time to reduce the influences of multiple factors from complex oral environments. Water-triggered character endows GCPC with the rapid transformation ability of mineral precursors to repair the enamel in a short time. In addition, the simple operations of GCPC in application will reduce the patient's visit time and discomfort in treatments, and it is feasible to be used in daily oral hygiene managements.

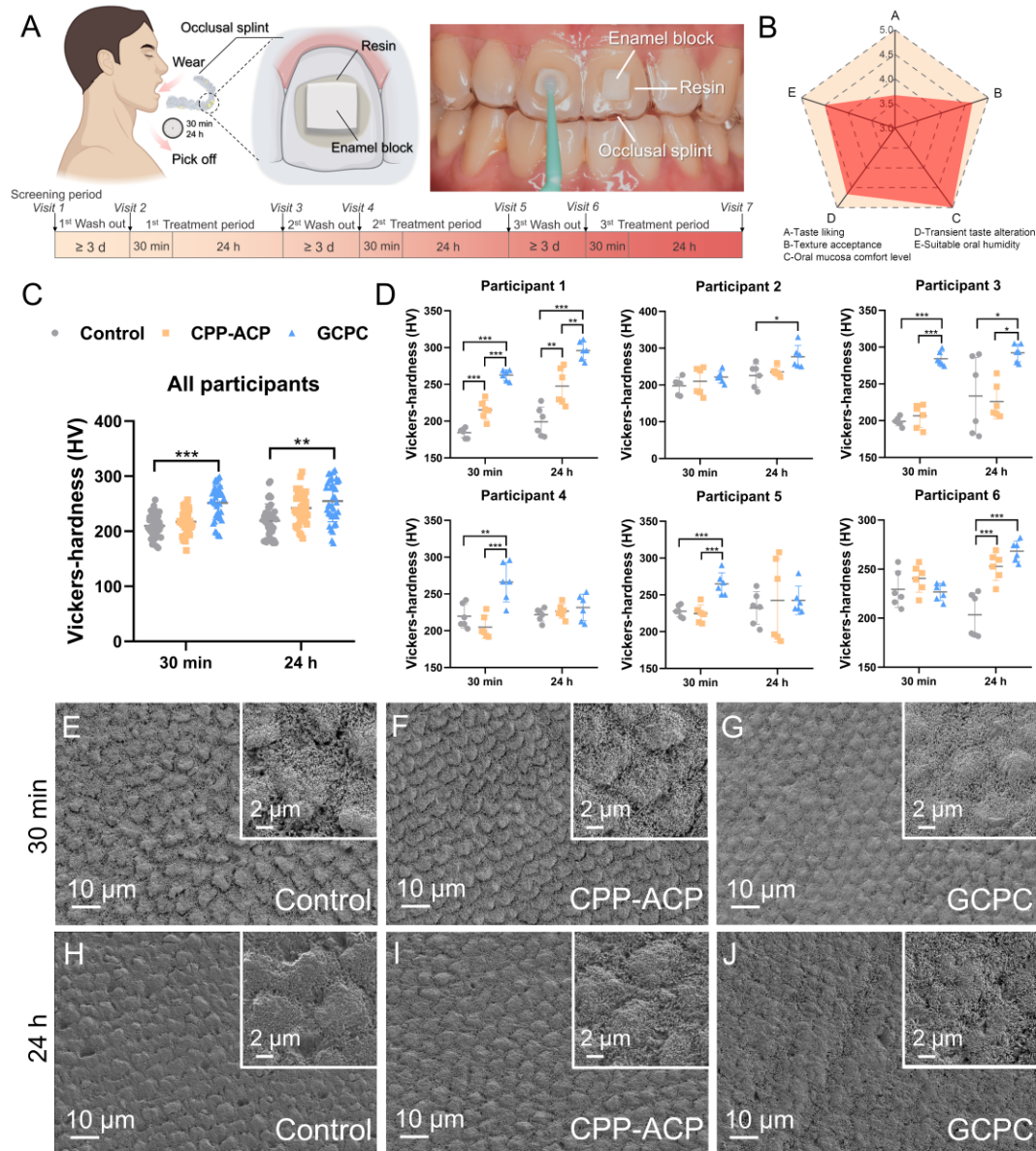


Fig. 7. The repair of demineralized enamel in clinical trial. (A) Schematic of clinical trial (left) and photograph (right) of an occlusal splint worn by a participant with etched enamels fixed on it. (B) Evaluation of sensory satisfaction by participants in terms of taste liking, texture acceptance, oral mucosa comfort level, transient taste alteration and suitable oral humidity. Score 1 to 5: very unsatisfied to very satisfied. Vertices on axes represent the mean of scores for n = 6. (C) Statistic analysis on the microhardness of repaired enamels carried by all participants. The error bars represent the mean \pm SD for n = 36, **p < 0.01, ***p < 0.001. (D) Microhardness of the repaired enamels carried by each participant in the clinical trial. The error bars represent the mean \pm SD for n = 6, *p < 0.05, **p < 0.01, ***p < 0.001. (E-G) SEM images of the enamel surfaces repaired by control sample (E), CPP-ACP paste (F) and GCPC (G) for 30 min in the clinical trial. (H-J) SEM images of the enamels repaired by control sample (H), CPP-ACP paste (I) and GCPC (J) for 24 h in the clinical trial.

Conclusion

In summary, we have developed a stable ultrasmall (1-2 nm) mineral species, GCPC, and find it can perform a rapid remineralization of tooth enamel by a water-triggered transformation. As an indispensable stabilizer, glycerol effectively stabilizes GCPC but endows it with the character of water-responsive transformation. On the etched enamel surface, GCPC can easily enter the nano-/micro-sized defect sites due to its small size and high permeability, then quickly repair it in the artificial saliva: with a continuous exchange between glycerol and water in high rate, GCPC forms amorphous calcium phosphate nanowires in 5 min, subsequently fuse and crystallize into compact HAP nanorods vertical to enamel surfaces in 10 min, and finish the transformation in 30 min, which is much faster than the conventional materials (hours or days). This remineralization behavior could expand the theory of nonclassical crystallization due to the special intermediate (ACP nanowire) and its crystallization behavior. No matter in the static and oscillated environments, GCPC constructs a dense mineral repair layer ultimately and recovers the mechanical properties to the values close to that of natural enamel, which is better than conventional remineralization commodities. In particular, the clinical trial study further confirms the desirable efficiency of GCPC in recovering enamel structure and mechanical properties. This biocompatible material, GCPC, is not only efficient in remineralization of etched enamels, but also advantageous in easy preparation process, low cost and simple conduction on enamel treatments, making it promising in future clinical promotion.

Experimental section

Materials and chemicals

Glycerol, hydroxyethyl piperazine ethane sulfonic acid (Hepes), sodium hydroxide and deuterium oxide were purchased from Shanghai Macklin Biochemical Technology Corporation, calcium chloride (CaCl_2), trisodium phosphate (Na_3PO_4), magnesium chloride (MgCl_2), potassium chloride (KCl), phosphoric acid and potassium dihydrogen phosphate (KH_2PO_4) were purchased from Aladdin Industrial Corporation. An oral health care paste product that is commonly used in enamel clinic remineralization treatment with CPP-ACP as the active substance was commercially purchased. Acetone and sodium fluoride (NaF) were purchased from Sinopharm Chemical Reagent Co. All chemicals were used as received without further purification. Human tooth samples were extracted following standard procedures for extraction at the Shanghai Ninth People's Hospital, and handled with permission of the Institutional Review Board (Approval No.:SH9H-2021-T445-2). The teeth were temporarily stored in sterile alcohol after removal.

Preparation of GCPC

At room temperature, 1.00 mmol of Na_3PO_4 was dissolved in mixed solvents of 3.00 mL of deionized water and 25.00 mL of glycerol. Under vigorous stirring, 2.00 mL of aqueous solution containing 1.50 mmol CaCl_2 was added dropwise into it, by which the solution became turbid and form GCPC in it. In this system, the Ca/P molar ratio was 1.5:1, and the volume content of water in solvents ($\text{water}/(\text{water}+\text{glycerol})$) was 16.7 v/v%. GCPC in the preparation solution without any separation is termed GCPC solution in this paper, which has only soluble NaCl as the byproduct.

The concentrations of Na_3PO_4 and CaCl_2 can be tripled while other conditions kept the same as above to prepare the 3X-GCPC. 3X-GCPC in the preparation solution without any separation is termed 3X-GCPC solution in this paper.

The amount of deionized water in the calcium and phosphorus salts solution was varied in equal proportion while maintaining a total volume of 30.0 mL to prepare GCPC solution with different water contents.

ACP in aqueous solution was prepared in deionized water by replacing all the glycerol with the same volume of water while other conditions kept the same as above.

Preparation of GCPC-ACP

To prepare GCPC-ACP, 5.00 mL of GCPC solution (water content 16.7 v/v%) was mixed with 50.00 mL of ethanol, then the resulting precipitation was centrifuged at 8000 rpm, washed with ethanol for 6 times and finally dried in an evacuated desiccator.

Repair of enamel using GCPC

Preparation of artificial saliva

Artificial saliva was prepared following the report⁴² using 0.07g CaCl_2 , 0.04g MgCl_2 , 2.23 g KCl , 0.54g KH_2PO_4 and 4.76 g HEPES in 1L of deionized water, whose pH was adjusted to 7.0 at 37 °C using NaOH solution.

Repair of demineralized enamels

Demineralized enamel, as a model of caries, was prepared by acid-etching the sound human enamel. Briefly, the dental crowns were cut with a low-speed wheel diamond saw (Model 971, JIAODA, China) into 3mm×3mm×5mm enamel blocks and embedded in resin while exposing only the top enamel surface. The exposed enamel surfaces were polished with silicon carbide paper to remove bacterium speckle and pigment, then immersed in 37wt% phosphoric acid for 60 s to partially demineralize the enamel. Finally, these specimens were washed with anhydrous ethanol and ultrapure water and dried at room temperature.

The demineralized enamels were treated with GCPC to evaluate its repair capacity. For each of demineralized enamel, half of its surface was coated with nail varnish as the non-treatment area, and the remaining half was treated with GCPC as the treatment area. After the nail varnish completely cured, the enamel was immersed into artificial saliva at 37 °C for 1 h to totally wet it like the teeth in oral environments. Without drying the surface, a drop of GCPC solution (water content 16.7 v/v%) was applied onto it using a micro brush (2.0mm, TISEN, Huanghua Promisee Dental Co., Ltd.), then brushed for 5 s, and incubated in artificial saliva at 37 °C again for certain time. After 24 h, the samples were taken out, flushed by water to remove the unbound materials on the surface, and treated with GCPC solution again as above. After further 24 h (48 h in total), the surface was cleaned again with flushing water, and dried at room temperature.

To investigate the repair effect at early time, after incubation of GCPC solution coated enamels in artificial saliva for 5 min, 10 min and 30 min, the samples were flushed with ethanol to quench the reaction and clean the surface, then dried at room temperature for characterization. In order to characterize the formed nanowires on enamel surface at 5 min, the GCPC repaired enamels were ultrasonicated for 30 s in ethanol, then the nanowires in ethanol were collected by standing for 30 min, and dropped on carbon coated copper grid for TEM observation after

being dried at room temperature.

To compare the repair effect of GCPC with other conventional materials, NaF and a commercial product with casein phosphopeptide-amorphous calcium phosphate (CPP-ACP) as the active substance were also used to treat the demineralized enamel. For NaF treatment, demineralized enamel was placed in artificial saliva containing 2wt% NaF; for CPP-ACP paste treatment, it was conducted via the same procedures as that of GCPC.

In addition, a hasher environment was used to investigate the repair effect. Based on the procedures above, during incubation of the GCPC coated enamel in artificial saliva at 37 °C, an oscillation at 80 rpm/min was applied in a thermostatic oscillator (ZHXY-50V, ZHICHU, China).

The transformation of GCPC on different substrates

Glass and HAP nanorod disks were used as the substrates to study the GCPC transformation on them.

For the preparation of HAP nanorods and disks, 2.317 g of CaCl_2 was dissolved in 250 mL of deionized water to prepare the solution of calcium source; 1.025g of Na_3PO_4 and 0.887g of Na_2HPO_4 were dissolved in 250 mL of deionized water to prepare the phosphorus source. Calcium source and phosphorus source solutions were mixed during vigorous stirring by a magnetic stirrer. Then the mixture solution was transferred into a glass bottle, sealed, and heated at 120 °C for 24 h. The products were washed with deionized water and ethanol for several times and dried at 60 °C. The HAP nanorod disk was prepared by pressing 200 mg of the dried HAP nanorods and using a powder tablet press (HY-15, TIANGUANG, China) at the pressure of 10 MPa.

For transformation study, like on enamel, GCPC was coated on the glass and HAP disks, and immersed in artificial saliva for certain time, then taken out and put into anhydrous ethanol to stop the reaction, finally dried in air at room temperature.

Characterizations.

The GCPC samples were characterized by spherical aberration corrected transmission electron microscope (ACTEM, JEM-ARM300F) equipped with the liquid cell holder (Protochips Poseidon 500). The relative quantification of turbidity was conducted by a microplate reader (Tecan Spark10M, Switzerland), by which 200 μL of each sample was added into a well of 96-well plates and the OD values were recorded at the wavelength of 590 nm. Repeat the test three times for each group. The compositions and structures of GCPC-ACP were characterized by Thermogravimetric-Flourier transform infrared spectroscopy (TGA-FTIR, TGA 8000-Front-Clarus 680-Clarus Sq 8T) and X-ray diffractometer (XRD, Rigaku Ultima IV, Japan).

^{31}P liquid nuclear magnetic resonance (NMR) characterization was conducted using a Bruker AVANCE NEO 700MHz at room temperature. Water in test samples was replaced with deuterium oxide. 300 scans were accumulated for ^{31}P NMR spectra of GCPC and the recycle delay was 4 s; 32 scans were accumulated for ^{31}P NMR spectra of Na_3PO_4 glycerol solution and the recycle delay was 2 s.

GCPC-ACP and nanowires on repaired enamel surface at 5 min were characterized by transmission electron microscopy (FEI Talos F200X). Enamel samples covered with nail

varnish were washed by acetone to remove it before SEM observation. The GCPC repaired enamels as well as the GCPC treated HAP nanorod disks and glass were characterized by scanning electron microscopy (Zeiss Gemini 450, Zeiss Gemini 300 and Navigator-100). A Knoop microhardness tester (HXD-1000 TMC, China) was used to assess the surface hardness of the samples with a load of 0.490 N applied for 15 s. Each one was tested for three times and the average value and standard deviation were recorded.

Cytotoxicity test

Human dental pulp stem cells (provided by Shanghai YSRIBIO industrial CO., LTD.) and Human oral keratinocytes (provided by Shanghai Engineering Research Center of Tooth Restoration and Regeneration) were cultured to logarithmic phase, then inoculated into 96-well plates and 24-well plates where they were soaked in complete medium (Dulbecco's modified Eagle's medium, Gibco, USA). The cells were incubated for 24 h to allow attachment. GCPC were incubated in complete medium with different concentrations (0, 12.5, 25, 50 mg/mL) for 24 h. The supernatants were collected by centrifugation at 3000 rpm for 5min and filtrated by syringe filter unit (SLGP033RB, Millipore), then added to each well in 24-well plates and 96-well plates. After certain intervals, CCK-8 and Live/dead staining assays were conducted as follows:

CCK-8 assay was assessed by a Cell Counting Kit-8 (CCK-8) (Beyotime, Shanghai, China). Briefly, 10 μ L CCK-8 solution was added to each well of 96-well plates, and incubated with the cells further for 2 h. The absorbance measurements were performed three times at the wavelength of 450 nm using a microplate reader (Tecan Spark10M, Switzerland).

Live/dead staining assay was conducted using a Calcein/PI Cell Viability/Cytotoxicity Assay Kit (Beyotime, Shanghai, China) in 24-well plates. Culture medium in the wells was removed and 250 μ L Calcein/PI working solution was added (prepared according to the kit instructions) to each well. The plates were incubated at 37 °C in the darkness for 30 min, then cells were imaged by inverted fluorescent microscope (Nikon Eclipse Ti-U, Japan). Green fluorescence corresponded to live cells and red fluorescence was related to dead cells.

Animal experiments.

Acid-etched enamel blocks were fixed in the maxilla of rats to evaluate the repair capacity of GCPC under in vivo mouth environments. Female Sprague-Dawley (SD) rats (8 weeks old, 200-280 g, 2 enamel block samples on each rat and 5 rats in each group) were chosen to conduct the animal experiments, which were approved by the Animal Experimental Ethics Committee of Shanghai Ninth People's Hospital. Two holes were symmetrically prepared on each enamel block for fixation in the rat mouths with a stainless steel ligature (diameter of 0.10 mm). Following the experimental procedures above, the surfaces of all samples were etched in 37wt% phosphoric acid to form artificial demineralized enamels, and half surface of each one was coated with nail varnish for comparison. One end of the stainless steel ligature was inserted into the interproximal space between the first and second maxillary molars, and the other end was connected to the upper central incisors. In this case, the enamel blocks were fixed in the anterior part of the maxilla where buccal muscles and lingual muscles moved frequently and often contacted enamel samples. Then they were treated with GCPC, CPP-ACP paste, and deionized water (blank) after enamel surface was wetted by saliva. After certain intervals, the enamel

samples were taken out, flushed by deionized water and dried at room temperature to assess the remineralization effect.

Clinical trials

Design of clinical trial

A double-blind, randomized and crossover in situ clinical trial was designed to study the performance of GCPC on enamel remineralization in human mouths. Both the research protocol and written informed consent were reviewed and approved by the Ethical Committee of Shanghai Ninth People's Hospital (No.: SH9H-2022-T31-1) prior to the study initiation. Generally healthy adults, consisting of 6 university students, were recruited for this clinical trial. Eligible participants had to be at least 18 years old, had at least 28 natural teeth (not including wisdom teeth). Subjects with any of the following conditions were not eligible for further study: untreated caries and pulpitis, severe periodontal diseases and salivary gland disorders; taking drugs that may affect the change of oral microbial flora (i.e., antibiotics) or inhibit the flow of saliva (i.e., antidepressants and antihistamines); suffering from bruxism and wearing fixed or invisible appliances. All the recruited participants received instructions of trial details and were informed of their possible benefits and risks. Then they signed the informed consent forms and their demographics and medical history were recorded.

To ensure that the participants, clinicians, laboratory technicians and statisticians were blinded to every treatment, all test agents (GCPC, CPP-ACP paste and control) were packaged identically and coded A, B or C by the additional study staff, who retained the code until the completion of the study and data interpretation. Six treatment sequences (A-B-C, A-C-B, B-A-C, B-C-A, C-A-B, C-B-A) were randomly assigned to the 6 recruited participants (one sequence for one participant). Human enamel blocks (3mm×3mm×2mm, prepared with the same approach as above) underwent acid etching in 37wt% phosphoric acid solution for 60 s to create a model of demineralized enamel, then were randomly attached to occlusal splints (each occlusal carries four blocks) which was subsequently worn in mouths of participants for tests. Participants were required to complete four study periods (7 visits in total), which include screening period, and three treatment (GCPC, CPP-ACP paste or control) periods in the assigned sequences. Each of study period was separated by a washout period of at least 3 d in which participants brush their teeth using the same fluoride-free toothpaste (Saky, China). After each treatment, the enamel specimens were removed from occlusal splint and collected for further laboratory assessments.

Preparation of GCPC for clinical trial

The GCPC used for clinical trials was formulated as above with a slight modification, whereby the phosphorus source was changed from Na_3PO_4 into the mixture of Na_2HPO_4 and Na_3PO_4 (molar ratio 4:1) without changing the total concentration of phosphorus source, and Ca/P molar ratio was decreased from 1.5 to 1.1 accordingly following the stoichiometry. This modification aimed to lower the pH of GCPC in water from 9.1 to 7.5 although the previous one did not show any negative effects during cell and animal tests. Preparation of GCPC used for clinical trials was entrusted to Hangzhou Jiaojie Oral Health Care Products Co., Ltd. In brief, 40.00 mmol of Na_2HPO_4 (>99.0%, pharmaceutical grade, Nanjing Chemical Reagent Co., Ltd) and 8.00 mmol of NaOH (>97.0%, pharmaceutical grade, Nanjing Chemical Reagent Co., Ltd)

were dissolved in 120.00 mL of ultrapure water to form the phosphorus source. Then 44.00 mmol of CaCl₂ (>97.0%, pharmaceutical grade, Hunan Xinlvfang Pharmaceutical Co., Ltd.) was dissolved in 80.00 mL of ultrapure water as the calcium source. At the mixing step, the phosphorus source was dispersed in 1.00 L of glycerol (99.9%, food grade, toothpaste raw material, Anjiruizhi Biotechnology Co., Ltd) followed by adding the calcium source under vigorous stirring. After further stirring for 20 minutes in vacuum (for removing air bubbles from the samples), the solution formed the GCPC in it.

For sample of control group, only 88.00 mmol NaCl (>99.1%, food grade, refined salt, China National Salt Industry Co., Ltd), identical to the byproduct in the GCPC production process, was dissolved in the mixed solvents of 200.00 mL of ultrapure water and 1.00 L of glycerol.

Occlusal splint manufacture

To protect the participants' natural dentition, occlusal splint was used to carry the demineralized human enamel blocks for trials. The maxillary impressions of each subject were taken using silicon rubber (DMG, Germany) to design the occlusal splint. The occlusal splint was fabricated with a 1.0 mm thick of splint hard material (Keystone, USA) and an air pressure machine (Druformat-TE, Germany). The human enamel blocks were irradiated by ⁶⁰Co (16kGy, 10MeV high-power electron linac, CGNPC) for sterilization, then immersed in 37wt% phosphoric acid for 60 s to partially demineralize the enamel. For each occlusal splint, four acid-etched enamel blocks were fixed on the buccal surfaces of the central incisors and first molars (2 on the left and 2 on the right) with flowable composite resin (Shofu, Japanese). All occlusal splints bonded with enamel blocks were sterilized with 75% alcohol before using for trials.

In situ experiment

The study investigator placed occlusal splints in the participant's mouth and brushed each enamel block with 30 μL (adsorbed in the micro brush with a diameter of 2mm purchased from Premium Plus (Dongguan) Ltd) of the prepared GCPC for 60 s. At 30 min, occlusal splints were removed (to obtain the specimens of 30 min). Afterwards, participants wore new occlusal splints, then the treatments on the enamel blocks were repeated and the enamel blocks were collected after 24 h (to obtain the specimens of 24 h). Participants were instructed to manage diets (avoid foods that could change the pH level of the mouth such as carbonated drinks and yogurt) and remove occlusal splints when they ate or drank and when they conducted their normal oral hygiene procedures. Adverse events and any abnormalities were recorded throughout the whole trial. An evaluation of sensory satisfaction of participants was carried out by using a questionnaire.

The collected enamel block specimens were characterized by a Knoop microhardness tester (HXD-1000 TMC, China) and scanning electron microscopy (Zeiss Gemini 300). Those at 24 h were soaked in DMSO (Aladdin, China) to remove bacteria and organic substances. Statistical analyses for all endpoints were performed using one-way ANOVA test and Bonferroni correction and the level of significance was set at 5 % ($p < 0.05$).

Acknowledgements

The financial support from the National Natural Science Foundation of China (31771081,

81300911 and 52272304), the Science and Technology Commission of Shanghai Municipality (21ZR1449700, 19441901900 and 22Y11903200), and Cross Research Fund of Ninth People's Hospital Affiliated to Shanghai Jiao Tong University, School of Medicine (JYJC202204) are gratefully acknowledged.

References

1. Bawaskar, H.S. & Bawaskar, P.H. Oral diseases: a global public health challenge. *Lancet* **395**, 185-186 (2020).
2. Moradian-Oldak, J. & George, A. Biom mineralization of Enamel and Dentin Mediated by Matrix Proteins. *J. Dent. Res.* **100**, 1020-1029 (2021).
3. Palmer, L.C., Newcomb, C.J., Kaltz, S.R., Spoerke, E.D. & Stupp, S.I. Biomimetic systems for hydroxyapatite mineralization inspired by bone and enamel. *Chem. Rev.* **108**, 4754-4783 (2008).
4. Du, C., Falini, G., Fermani, S., Abbott, C. & Moradian-Oldak, J. Supramolecular assembly of amelogenin nanospheres into birefringent microribbons. *Science* **307**, 1450-1454 (2005).
5. Fan, Y., Sun, Z. & Moradian-Oldak, J. Controlled remineralization of enamel in the presence of amelogenin and fluoride. *Biomaterials* **30**, 478-483 (2009).
6. Cross, K.J., Huq, N.L. & Reynolds, E.C. Casein phosphopeptides in oral health--chemistry and clinical applications. *Curr. Pharm. Des.* **13**, 793-800 (2007).
7. Wang, D., *et al.* Controlling Enamel Remineralization by Amyloid-Like Amelogenin Mimics. *Adv. Mater.* **32**, e2002080 (2020).
8. Shao, C., *et al.* Repair of tooth enamel by a biomimetic mineralization frontier ensuring epitaxial growth. *Sci. Adv.* **5**, eaaw9569 (2019).
9. Li, L., *et al.* Bio-inspired enamel repair via Glu-directed assembly of apatite nanoparticles: an approach to biomaterials with optimal characteristics. *Adv. Mater.* **23**, 4695-4701 (2011).
10. Chang, R., *et al.* Phosphorylated and Phosphonated Low-Complexity Protein Segments for Biomimetic Mineralization and Repair of Tooth Enamel. *Adv. Sci.* **9**, e2103829 (2022).
11. Habraken, W.J., *et al.* Ion-association complexes unite classical and non-classical theories for the biomimetic nucleation of calcium phosphate. *Nat. Commun.* **4**, 1507 (2013).
12. Gebauer, D., Kellermeier, M., Gale, J.D., Bergström, L. & Cölfen, H. Pre-nucleation clusters as solute precursors in crystallisation. *Chem. Soc. Rev.* **43**, 2348-2371 (2014).
13. Dey, A., *et al.* The role of prenucleation clusters in surface-induced calcium phosphate crystallization. *Nat. Mater.* **9**, 1010-1014 (2010).
14. Gower, L.B. Biomimetic model systems for investigating the amorphous precursor pathway and its role in biom mineralization. *Chem. Rev.* **108**, 4551-4627 (2008).
15. Olszta, M.J., *et al.* Bone structure and formation: A new perspective. *Mater. Sci. Eng., R* **58**, 77-116 (2007).
16. Veis, A. & Dorvee, J.R. Biom mineralization mechanisms: a new paradigm for crystal nucleation in organic matrices. *Calcif. Tissue Int.* **93**, 307-315 (2013).
17. Onuma, K. & Ito, A. Cluster Growth Model for Hydroxyapatite. *Chem. Mater.* **10**, 3346-3351 (1998).
18. Park, J., *et al.* Quantitative Analysis of Calcium Phosphate Nanocluster Growth Using Time-of-Flight Medium-Energy-Ion-Scattering Spectroscopy. *ACS Cent. Sci.* **4**, 1253-1260 (2018).
19. Lotsari, A., Rajasekharan, A.K., Halvarsson, M. & Andersson, M. Transformation of

- amorphous calcium phosphate to bone-like apatite. *Nat. Commun.* **9**, 4170 (2018).
20. De Yoreo, J.J., *et al.* CRYSTAL GROWTH. Crystallization by particle attachment in synthetic, biogenic, and geologic environments. *Science* **349**, aaa6760 (2015).
21. Kim, S., Ryu, H.-S., Shin, H., Jung, H.S. & Hong, K.S. In situ observation of hydroxyapatite nanocrystal formation from amorphous calcium phosphate in calcium-rich solutions. *Mater. Chem. Phys.* **91**, 500-506 (2005).
22. Yao, S., *et al.* Biomineralization: From Material Tactics to Biological Strategy. *Adv. Mater.* **29**(2017).
23. Xiao, Z., *et al.* Rapid biomimetic remineralization of the demineralized enamel surface using nano-particles of amorphous calcium phosphate guided by chimaeric peptides. *Dent. Mater.* **33**, 1217-1228 (2017).
24. He, J., *et al.* Polyzwitterion Manipulates Remineralization and Antibiofilm Functions against Dental Demineralization. *ACS Nano* (2022).
25. Babaie, E., *et al.* Polymer-Induced Liquid Precursor (PILP) remineralization of artificial and natural dentin carious lesions evaluated by nanoindentation and microcomputed tomography. *J. Dent.* **109**, 103659 (2021).
26. Zhou, C.H., Beltrami, J.N., Fan, Y.X. & Lu, G.Q. Chemoselective catalytic conversion of glycerol as a biorenewable source to valuable commodity chemicals. *Chem. Soc. Rev.* **37**, 527-549 (2008).
27. Robergs, R.A. & Griffin, S.E. Glycerol. Biochemistry, pharmacokinetics and clinical and practical applications. *Sports Med.* **26**, 145-167 (1998).
28. He, K., *et al.* Revealing nanoscale mineralization pathways of hydroxyapatite using in situ liquid cell transmission electron microscopy. *Sci. Adv.* **6**(2020).
29. Li, N., *et al.* Biomimetic inorganic-organic hybrid nanoparticles from magnesium-substituted amorphous calcium phosphate clusters and polyacrylic acid molecules. *Bioact. Mater.* **6**, 2303-2314 (2021).
30. Vecstaudza, J., Gasik, M. & Locs, J. Amorphous calcium phosphate materials: Formation, structure and thermal behaviour. *J. Eur. Ceram. Soc.* **39**, 1642-1649 (2019).
31. Mu, Z., *et al.* Pressure-driven fusion of amorphous particles into integrated monoliths. *Science* **372**, 1466-1470 (2021).
32. Zhang, H., De Yoreo, J.J. & Banfield, J.F. A unified description of attachment-based crystal growth. *ACS Nano* **8**, 6526-6530 (2014).
33. Sun, S., Gebauer, D. & Cölfen, H. Alignment of Amorphous Iron Oxide Clusters: A Non-Classical Mechanism for Magnetite Formation. *Angew. Chem. Int. Ed. Engl.* **56**, 4042-4046 (2017).
34. Jehannin, M., Rao, A. & Cölfen, H. New Horizons of Nonclassical Crystallization. *J. Am. Chem. Soc.* **141**, 10120-10136 (2019).
35. Yang, Y., *et al.* Determining the three-dimensional atomic structure of an amorphous solid. *Nature* **592**, 60-64 (2021).
36. Bai, Y., *et al.* Protein nanoribbons template enamel mineralization. *Proc. Natl. Acad. Sci. U. S. A.* **117**, 19201-19208 (2020).
37. Rodriguez-Navarro, C., Burgos Cara, A., Elert, K., Putnis, C.V. & Ruiz-Agudo, E. Direct Nanoscale Imaging Reveals the Growth of Calcite Crystals via Amorphous Nanoparticles. *Cryst. Growth Des.* **16**, 1850-1860 (2016).

38. Jin, B., *et al.* Anisotropic Epitaxial Behavior in the Amorphous Phase-Mediated Hydroxyapatite Crystallization Process: A New Understanding of Orientation Control. *J. Phys. Chem. Lett.* **10**, 7611-7616 (2019).
39. Prajapati, S., Ruan, Q., Mukherjee, K., Nutt, S. & Moradian-Oldak, J. The Presence of MMP-20 Reinforces Biomimetic Enamel Regrowth. *J. Dent. Res.* **97**, 84-90 (2018).
40. Fang, Z., *et al.* Enamel-like tissue regeneration by using biomimetic enamel matrix proteins. *Int. J. Biol. Macromol.* **183**, 2131-2141 (2021).
41. Creeth, J.E., *et al.* Dose-response effect of fluoride dentifrice on remineralisation and further demineralisation of erosive lesions: A randomised in situ clinical study. *J. Dent.* **43**, 823-831 (2015).
42. Cao, G., *et al.* Antibacterial silver-doped calcium phosphate synthesized by an enzymatic strategy for initial caries treatment. *Ceram. Int.* **46**, 22466-22473 (2020).